

RSC Advances



This is an *Accepted Manuscript*, which has been through the Royal Society of Chemistry peer review process and has been accepted for publication.

Accepted Manuscripts are published online shortly after acceptance, before technical editing, formatting and proof reading. Using this free service, authors can make their results available to the community, in citable form, before we publish the edited article. This *Accepted Manuscript* will be replaced by the edited, formatted and paginated article as soon as this is available.

You can find more information about *Accepted Manuscripts* in the [Information for Authors](#).

Please note that technical editing may introduce minor changes to the text and/or graphics, which may alter content. The journal's standard [Terms & Conditions](#) and the [Ethical guidelines](#) still apply. In no event shall the Royal Society of Chemistry be held responsible for any errors or omissions in this *Accepted Manuscript* or any consequences arising from the use of any information it contains.



Self-assembly of amine-functionalized gold nanoparticle on phosphonate-functionalized graphene nanosheet: A highly active catalyst for reduction of 4-nitrophenol†

Received 00th January 20xx,
Accepted 00th January 20xx

DOI: 10.1039/x0xx00000x

www.rsc.org/

Xueqing Gao^{‡,a}, Guangrui Xu^{‡,b}, Zhao Yan^c, Shuni Li^{*,a}, Feng Shi^{*,b} and Yu Chen^b

The graphene nanosheet (GNS) supported gold nanoparticle (Au-NP) composites (Au-NP/GNS) have attracted wide attention due to their important applications in catalysis, sensing, optics, medicine, and fuel cells. In this work, based on the strong electrostatic and/or hydrogen bonding interactions between amine-functionalized Au-NP (Au-NP@NH₂) and phosphonate-functionalized GNS (GNS-PO₃H₂), a self-assembly strategy is used to synthesize Au-NP/GNS composites. The physical and chemical properties of Au-NP@NH₂, GNS-PO₃H₂, and Au-NP/GNS composites are fully investigated by various physical characterizations, including X-ray powder diffraction, X-ray photoelectron spectroscopy, ultraviolet-visible spectroscopy, transmission electron microscopy, and zeta potential analysis. The experimental results demonstrate the phosphonate-functionalization of GNS is critical for the generation of the high-quality Au-NP/GNS composites. The as-prepared Au-NP/GNS composites show the improved catalytic activity for the degradation of 4-nitrophenol compared to functionalized Au-NP, which is ascribed to the amine-functionalization of Au-NP and the introduction of GNS with high electrical conductivity and big surface area.

Introduction

The chemical functionalized gold nanoparticle (Au-NP), consisting of a small Au-NP core and a monolayer of functional molecule, has attracted much attention in field of catalysis, sensor and medicine due to its unique physical and chemical properties imparted by functional molecule.¹⁻⁶ For example, the apo-glucose dehydrogenase enzyme could reconstitute on pyrroloquinoline quinone functionalized Au-NP, which displayed the excellent bioelectrocatalytic activity for the glucose oxidation.² Bipyridine functionalized Au-NP could interact with Eu^{III}/Tb^{III} ions to yield phosphorescent nanomaterials.³ Polyvalent DNA-functionalized Au-NP selectively enhanced ribonuclease H activity, making DNA-functionalized Au-NP ideal gene regulation agents.⁴ Glutathione functionalized Au-NP could serve as carrier of platinum(IV) drug for prostate cancer treatment.⁵ Flavin-functionalized Au-NP could act as an efficient catalyst for aerobic organic transformations.⁶

It is well known that support materials generally affect the catalytic activity and stability of metal NP.⁷⁻¹³ Recent reports

demonstrate the two-dimensional graphene nanosheets (GNS) have high surface area as well as excellent mechanical and electronic properties, which make it a promising support material for the anchorage of metal NP.¹⁴⁻¹⁹ During the catalytic reaction, the high electrical conductivity of GNS facilitates the electron transfer. Meanwhile, the big surface area of GNS efficiently decreases the aggregation of metal NP. The two favorable factors improve the catalytic activity and stability of metal NP.¹⁵⁻¹⁹ Consequently, the considerable efforts have been made to incorporate Au-NP into GNS matrix and explore their potential applications in photothermal energy conversion,²⁰ plasmonic devices,²¹ photoacoustic imaging,²² photothermal therapy,²³ surface-enhanced Raman scattering,²⁴⁻²⁹ organic photovoltaic devices,³⁰ fuel cells,³¹⁻³⁵ heterogeneous catalysis,^{36, 37} and electrochemical sensors,³⁸⁻⁴³ *etc.* At present, the self-assembly method is an efficient strategy for the synthesis of Au-NP/GNS composites.^{23, 25, 26, 32, 36, 40} However, GNS tends to the irreversible aggregation in aqueous solution due to the strong π - π stacking and the pristine surface of GNS lacks the enough active sites for the anchorage of metal NP.²⁷ Therefore, the various aromatic molecules with amino groups,⁴⁴⁻⁴⁶ sulfonic groups,⁴⁷⁻⁵⁰ and carboxyl groups^{51, 52} have widely been used to functionalize GNS. Although phosphonic acid groups (-PO₃H₂) with the dibasic nature have good biocompatibility, high hydrophilicity, adjustable charge density, and strong coordination ability,⁵³⁻⁵⁶ little attention has been paid to the phosphonate-functionalization of GNS until now.

4-nitrophenol (4-NP), one of the most common nitroaromatic compounds, is widely used in the industrial synthesis, and has big solubility and high chemical stability in water.⁵⁷⁻⁶² The ingestion of 4-NP has been linked to several public health problems such as fever, ferverescence, methemoglobinemia, and liver and kidney damage

^a Key Laboratory of Macromolecular Science of Shaanxi Province, School of Chemistry & Chemical Engineering, Shaanxi Normal University, Xi'an 710062, PR China

E-mail: lishuni@snnu.edu.cn (S. Li)

^b School of Materials Science and Engineering, Shaanxi Normal University, Xi'an 710062, PR China

E-mail: shifeng@snnu.edu.cn (F. Shi)

^c National Coal Inspection Centre, Shaanxi Institute of Energy Quality Supervision and Inspection, Xi'an, Shaanxi, 710054, PR China

† Electronic Supplementary Information (ESI) available: Experimental Details. See DOI: 10.1039/c000000x

‡ These two authors made an equal contribution to this work.

Thus, 4-NP is regarded as highly hazardous and toxic pollutants by the US Environmental Protection Agency.⁵⁷ For remediating 4-NP contamination, the reductive transformation of 4-NP to less toxic 4-aminophenol (4-AP) is a simple and efficient method.^{58, 59, 63-66} Till now, Au-catalyzed reduction of 4-NP by NaBH₄ has been extensively investigated due to the high catalytic activity of Au-NP.^{57, 58, 60, 62, 67, 68} However, the effect of surface groups at Au-NP on catalytic activity of Au-NP is rarely reported.

In the work, we successfully synthesize amine-functionalized Au-NP composites (Au-NP@NH₂) by using polyethyleneimine (PEI, Fig. 1) as reducing agent and stabilizing agent, which shows remarkably improved catalytic activity for 4-NP reduction compared to carboxylate-functionalized Au-NP composites (Au-NP@COOH). Meanwhile, the phosphonate-functionalized GNS composites (GNS-PO₃H₂) are obtained easily based on the π - π stacking interaction between zoledronic acid (ZDA, Fig. 1) and GNS. Furthermore, Au-NP@NH₂ can efficiently self-assemble on GNS-PO₃H₂ surface due to the strong electrostatic and/or hydrogen bonding interactions. The introduction of GNS further enhances the catalytic activity of Au-NP@NH₂ for the 4-NP reduction.

Experimental

Reagents and chemicals

PEI (Mw \approx 600) is obtained from Aladdin Industrial Corporation. Graphene nanosheet (GNS) was purchased from Nanjing XFNANO Materials TECH Co., Ltd. Zoledronic acid (ZDA, Fig. 1), hydrogen tetrachloroaurate(III) tetrahydrate (HAuCl₄·4H₂O), 4-nitrophenol (4-NP), and sodium borohydride (NaBH₄) were purchased from Sinopharm Chemical Reagent Co., Ltd.

Synthesis of Au-NP@NH₂ and Au-NP@COOH

Au-NP@NH₂ composites were synthesized by using PEI as reducing agent and stabilizing agent at room temperature (Fig. 1A). In a typical synthesis, 1.0 mL of 24.2 mM HAuCl₄ solution was added into 41.0 mL of 12.1 mM PEI aqueous solution. After adjusting solution pH to 3.7, the mixture solution stands for 2 h at room temperature until the color of the mixture solution changes to red color.

For comparison, 13.0 nm Au-NP@COOH composites (ESI[†] Fig. S1, zeta potential: -42.9 mV at pH 4.8) were synthesized by sodium citrate reduction method.⁶⁹ In a typical synthesis, 30.0 mL of 0.4 mM HAuCl₄ aqueous solution was put into a three-neck flask equipped with a reflux condense and heated to 100 °C. Then, 0.5 mL of 0.2 M sodium citrate solution was added rapidly into HAuCl₄ aqueous solution. The reaction was allowed to run until the solution became wine red color.

Synthesis of GNS-PO₃H₂

GNS-PO₃H₂ composites were synthesized by the π - π stacking interaction between GNS and ZDA (Scheme 1B). In a typical procedure, 10 mg of GNS was dispersed in 50 mL of 8.7 mM ZDA solution (pH 8.5) by ultrasonic treatment for 30 min. Then, GNS-PO₃H₂ were separated by centrifugation.

Synthesis of Au-NPs@NH₂/GNS-PO₃H₂ composites

Au-NPs@NH₂/GNS-PO₃H₂ composites were obtained by self-assembly of Au-NP@NH₂ on GNS-PO₃H₂ surface (Fig. 1C). In

a typical procedure, 21.0 mL of 0.1 mg mL⁻¹ Au-NP@NH₂ solution was added into 10.0 mL of 1.0 mg mL⁻¹ GNS-PO₃H₂ suspension with ultrasonic treatment for 60 min at room temperature. After self-assembly, Au-NPs@NH₂/GNS-PO₃H₂ composites were separated by centrifugation/washing cycles and then dried in a vacuum dryer. ICP-AES analysis shows Au-NPs@NH₂/GNS-PO₃H₂ composites contain 36.5 wt.% metal Au.

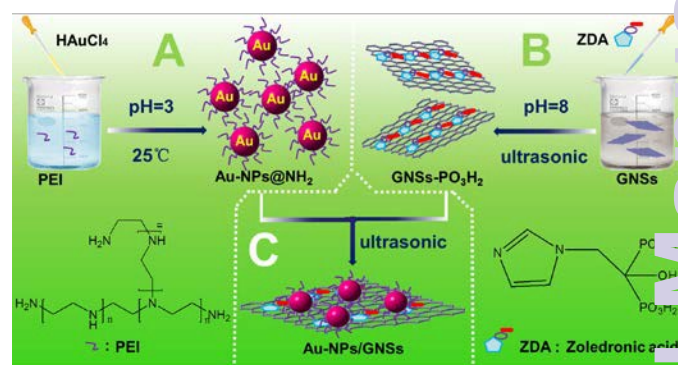


Fig. 1 Schematic synthetic route of Au-NPs@NH₂/GNS-PO₃H₂ composites.

Catalytic reduction of 4-NP

For catalytic reduction of 4-NP to 4-aminophenol (4-AP), 2.7 mL of 0.037 M NaBH₄ was added into 0.3 mL of 2.0 \times 10⁻³ M 4-NP aqueous solution. Then, 15.0 μ L of Au-NPs@NH₂/GNS-PO₃H₂ composites (0.3 g L⁻¹) aqueous suspension was added into the above solution at room temperature. The reaction progress was monitored by time-dependent ultraviolet-visible spectroscopy (UV-vis).

For comparison, Au-NP@NH₂ and Au-NP@COOH composites were also used as heterogeneous catalysts for the 4-NP reduction by using the same experimental procedure and reagent concentrations (including concentration of Au-NP) as those employed for Au-NPs@NH₂/GNS-PO₃H₂ composites.

Instruments

X-ray powder diffraction (XRD, Model D/max-rC), X-ray photoelectron spectroscopy (XPS, AXIS ULTRA), transmission electron microscopy (TEM, EOL JEM-2100F), and zeta potential analyzer (Malvern Zetasizer Nano ZS90) were used to investigate the structure, surface composition, morphology and surface charge of samples. Scanning electron microscopy-energy dispersive spectroscopy (SEM-EDX, FEI Quanta 200) and scanning transmission electron microscopy-energy dispersive spectroscopy (STEM-EDX, EOL JEM-2100F) were used to investigate the element distribution of samples. The accurate Au loading in Au-NPs@NH₂/GNS-PO₃H₂ composites was determined with an inductively coupled plasma atomic emission spectrometry (ICP-AES, Prodigy 7). UV-vis (UV2600) was used to monitor the real-time variation of the concentration of 4-NP.

Results and discussion

Characterization of Au-NPs@NH₂

The reduction of HAuCl₄ was first confirmed by color change of

solution (Fig. 2A). After adjusting the solution pH to 3.7, a sequence of color changes was observed and a wine-red color solution was obtained finally at 2 h, indicating the formation of stable Au-NP. The interaction between HAuCl₄ and PEI was further investigated by UV-vis measurement (Fig. 2B). As the reaction progresses, the plasmon peak of Au-NP around 528 nm gradually increases with time, which is characteristic of spherical Au-NP.⁷⁰ At 2 h, plasmon peak value of Au-NP reaches a maximum value and peak position fixes finally at 526 nm, implying the HAuCl₄ has been reduced completely by PEI. After storage for two months, UV-vis spectrum of Au-NP@NH₂ composites remains constant (data not shown), indicating PEI also efficiently acts as stabilizing agent.

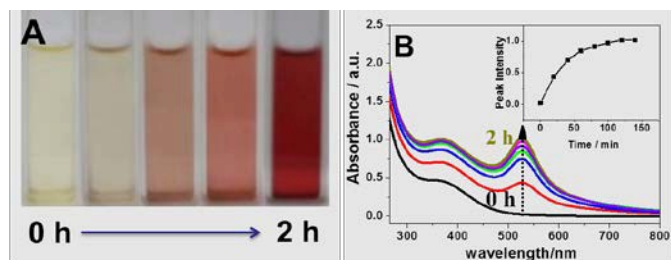


Fig. 2 (A) Photographs and (B) UV-vis spectra of HAuCl₄ and PEI mixture solution at different reaction time. Insert: the plot of the absorbance intensity around 528 nm as a function of time.

The crystal structure and chemical composition of Au-NP@NH₂ composites were investigated by XRD and XPS. The XRD pattern shows clearly the four diffraction peaks at 38.3, 44.4, 64.7 and 77.7° (Fig. 3A), which agrees well with standard diffraction data of face-centered cubic (*fcc*) Au crystal (JCPDS standard 04-0784). The binding energies of Au4f_{5/2} and Au4f_{7/2} locate at 86.8 and 83.1 eV (Fig. 3B), which are typical values of metallic Au. This fact further confirms the HAuCl₄ is reduced completely by PEI. Importantly, N1s signal at 399.6 eV is detected for Au-NP@NH₂ composites (Fig. 3B), originating from the -NH₂ groups at PEI. The appearance of N1s peak indicates the adsorption of PEI on Au-NP surface. Furthermore, the zeta potential of Au-NP@NH₂ composites is measured to be +49 mV at pH 5.0. It is clear that -NH₂ group will be protonated due to its nature of weak base. Thus, the positive zeta potential value of Au-NP@NH₂ composites confirms the PEI functionalization of Au-NP.

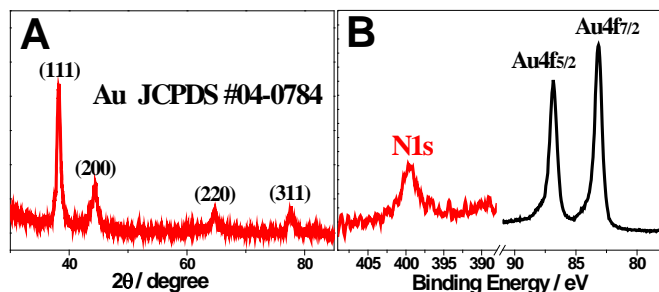


Fig. 3 (A) XRD pattern of Au-NPs@NH₂ and (B) XPS spectra of Au-NPs@NH₂ in the N1s and Au4f regions.

The morphology and size distribution of Au-NP@NH₂ composites were characterized by TEM. As observed, all particles are nearly spherical and well separated from each other (Fig. 4A). Selected area

electron diffraction (SAED) image shows irregular spot pattern (insert in Fig. 4A), implying their polycrystalline property. According to the size distribution histogram (Fig. 4B), the average size of Au-NP@NH₂ is estimated to be 33 nm. The high resolution TEM (HRTEM) image of an individual Au-NP@NH₂ particle shows clear lattice fringes (Fig. 4C). In further magnified HRTEM images, the Au (111) planes with d-spacing of 0.24 nm and Au (100) planes with d-spacing of 0.21 nm are observed (Fig. 4D), confirming their polycrystalline nature. EDX element mapping measurements show that N element pattern is very similar to Pt element pattern (Fig. 4F), demonstrating the uniform distribution of PEI on the surface of Au-NP.

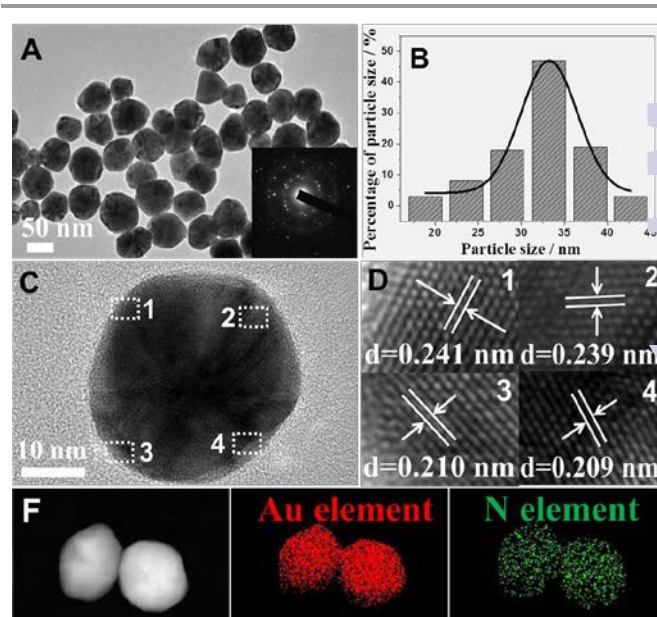


Fig. 4 (A) Typical TEM image of Au-NPs@NH₂. Insert: the SAED pattern of Au-NPs@NH₂. (B) The size distribution histogram of Au-NPs@NH₂. (C) HRTEM image of an individual Au-NPs@NH₂. (D) Magnified HRTEM images taken from regions (1, 2, 3, and 4) marked by white squares in (C), respectively. (E) High-angle annular dark-field scanning TEM image of Au-NPs@NH₂ and corresponding EDX element mapping patterns.

Characterization of GNS-PO₃H₂

The π - π stacking interaction between ZDA and GNS was confirmed by UV-Vis spectra (Fig. 5A). GNS has no obvious absorption peak in the range of 200-600 nm whereas ZDA has a strong absorption peak at 209 nm. Meanwhile, GNS-PO₃H₂ composites show the obvious peak at 211 nm, corresponding to ZDA with redshifts (ca. 2 nm). The appearance of characteristic peak of ZDA and its redshift suggest the successful functionalization of GO by ZDA.⁷¹ The phosphonate-functionalization of GNS was further chemically confirmed by XPS (Fig. 5B). The appearance of the characteristic N1s peak at 401.2 eV and P2p peak at 134.1 eV demonstrate the successful self-assembly of ZDA on GNS surface via π - π stacking interaction. The distribution of ZDA on GNS surface was investigated by EDX element mapping (Fig. 5C). As observed, C, N, and P elements distribute evenly on the same region, demonstrating the uniform distribution of ZDA on the GNS surface. Meanwhile the zeta potential of GNS-PO₃H₂ composites is measured to be -18.6 mV at pH 5.0, indicating negatively charged phosphonate groups are exposed to the outside of GNS.

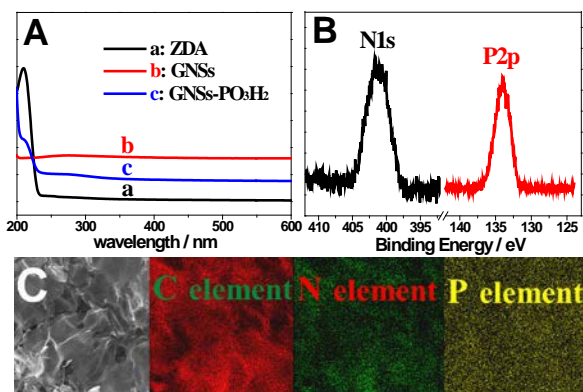


Fig. 5 (A) UV-vis spectra of (a) ZDA, (b) GNS and (c) GNS-PO₃H₂. (B) N1s and P2p XPS spectra of GNS-PO₃H₂. (C) Representative SEM image of GNS-PO₃H₂ and corresponding EDX element mapping.

Characterization of Au-NPs@NH₂/GNS-PO₃H₂ composites

Due to the strong electrostatic and/or hydrogen bonding interactions between -PO₃H₂ groups and -NH₂ groups,⁷²⁻⁷⁴ Au-NP@NH₂ can anchor easily on the GNS-PO₃H₂ surface via self-assembly. As observed, the wine-red color of Au-NP@NH₂ and GNS-PO₃H₂ mixture solution completely disappears after sonicating for 0.5 h (Fig. 6A), indicating the efficient anchorage of Au-NP@NH₂ on the GNS-PO₃H₂ surface. In contrast, the wine-red color of Au-NP@NH₂ and pristine GNS mixture solution still retains after sonicating for 0.5 h (Fig. 6B), indicating Au-NP@NH₂ can't completely anchor on the pristine GNS surface due to the absence of interaction. The self-assembly of Au-NP@NH₂ on GNS-PO₃H₂ was confirmed by TEM. As observed, the spherical Au-NP@NH₂ are uniformly dispersed on GNS-PO₃H₂ surface (Fig. 7A). In contrast, the few Au-NP@NH₂ anchor on the pristine GNS surface (Fig. 7B), in consistent with above-mentioned experimental observation. These experimental results confirm the phosphonate-functionalization of GNS facilitates the anchorage of Au-NP@NH₂, originating from the strong electrostatic and/or hydrogen bonding interactions.

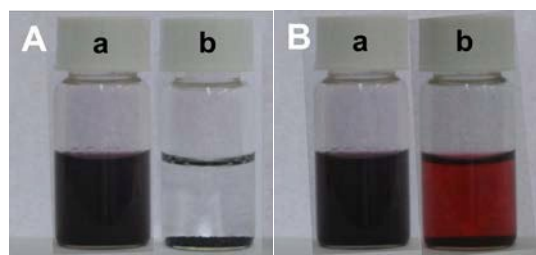


Fig. 6 (A) Photographs of Au-NPs@NH₂ and GNS-PO₃H₂ mixture solution (a) before and (b) after sonicating for 30min. (B) Photographs of Au-NPs@NH₂ and pristine GNS mixture solution (a) before and (b) after sonicating for 30 min.

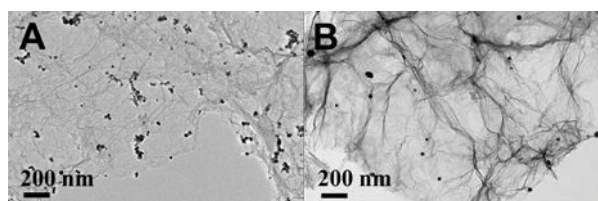


Fig. 7 Representative TEM images of the obtained Au-NPs@NH₂/GNS-PO₃H₂ composites by using (A) GNS-PO₃H₂ and (B) pristine GNS as support materials.

Catalytic activity of Au-NPs@NH₂/GNS-PO₃H₂ composites

The catalytic activity of Au-NPs@NH₂/GNS-PO₃H₂ composites for 4-NP reduction was investigated by time-dependent UV-vis spectra.⁷⁵⁻⁷⁹ For comparison, the catalytic activities of Au-NP@NH₂ and Au-NP@COOH composites were also evaluated. In the 4-NP/NaBH₄ reaction system, the absorbance peak at 400 nm is characteristic absorbance peak of 4-nitrophenolate in alkaline solution.^{80, 81} UV-vis spectra of 4-NP/NaBH₄ mixture remain constant within 4 h, indicating the reduction of 4-NP can't be completed in the absence of the catalyst (data not shown). Upon the introduction of Au-NP@NH₂, Au-NP@COOH, and Au-NPs@NH₂/GNS-PO₃H₂ composites into the reaction solution, however, the absorbance peak of 4-nitrophenolate decreases gradually with time and disappears finally, indicating the complete conversion of 4-NP to 4-AP (Fig. 8A-C). Au-NP@NH₂-catalyzed reduction of 4-NP is finished within 14 min (Fig. 8A), which is much shorter than Au-NP@COOH-catalyzed reduction of 4-NP with 20 min (Fig. 8B). Mainly, the positively charged Au-NP@NH₂ can sufficiently attract the negatively charged nitrophenolate and BH₄⁻ ions through electrostatic interaction, resulting in their enrichment on Au-NP surface. Furthermore, it is observed that Au-NPs@NH₂/GNS-PO₃H₂-catalytic reduction of 4-NP is finished within 7 min (Fig. 8C), showing an enhanced catalytic activity compared to Au-NP@NH₂ (Fig. 8A). According to the linear plots of ln(Ct/C0) versus time *t* (inserts in Fig. 8A-C),^{80, 81} the reaction rate constants are calculated to be 0.19, 0.126, and 0.325 min⁻¹ for the 4-NP reduction reactions catalyzed by Au-NP@NH₂, Au-NP@COOH and Au-NPs@NH₂/GNS-PO₃H₂, respectively.

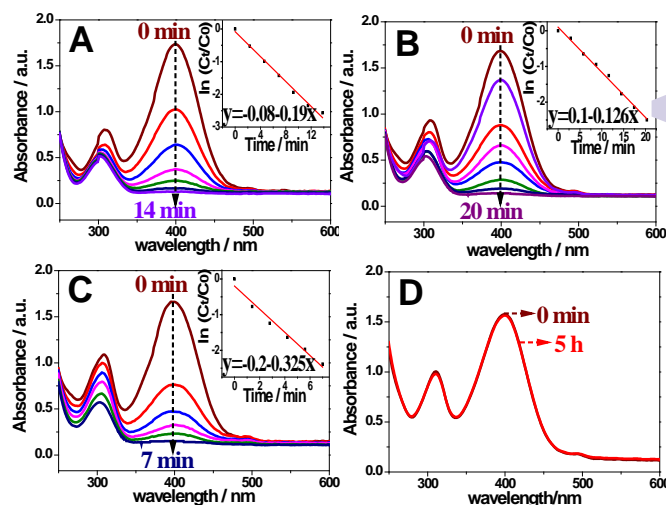


Fig. 8 UV-vis spectra for successive reduction of 4-NP with NaBH₄ using (A) Au-NPs@NH₂, (B) Au-NPs@COOH, (C) Au-NPs@NH₂/GNS-PO₃H₂, and (D) GNS-PO₃H₂ as catalysts.

Since GNS-PO₃H₂ don't show obvious catalytic behaviour for the reduction of 4-NP within 5 h (Fig. 8D), the enhanced catalytic activity of Au-NPs@NH₂/GNS-PO₃H₂ composites can be ascribed to the synergistic effect between Au-NP@NH₂ and GNS-PO₃H₂. On one hand, the highly conjugated sp² network of GNS provides excellent electrical conductivity for composites, which accelerates electron transfer in the course of 4-NP reduction. On the other hand, the introduction of GNS efficiently avoids the aggregation of Au-NP

in the course of 4-NP reduction, which also contributes to the improved catalytic activity of Au-NPs@NH₂/GNS-PO₃H₂ composites. Of course, the adsorption of substrate molecule on the GNS support with high surface area also likely facilitates the catalytic reduction of 4-NP.⁸² Subsequently, the recyclability of Au-NPs@NH₂/GNS-PO₃H₂ composites for 4-NP reduction was also investigated by repeatedly adding the 4-NP solution. After undergoing six catalysis cycles, Au-NPs@NH₂/GNS-PO₃H₂ composites exhibit almost constant catalytic activity for 4-NP reduction within 7 min, indicating Au-NPs@NH₂/GNS-PO₃H₂ composites possess good stability.

Conclusions

We have successfully synthesized Au-NP@NH₂ and GNS-PO₃H₂ composites. By means of strong electrostatic and/or hydrogen bonding interactions between -PO₃H₂ groups and -NH₂ groups, Au-NP@NH₂ can effectively self-assemble on the GNS-PO₃H₂ surface to generate the high-quality Au-NP/GNS composites. On the one hand, the PEI-functionalization of Au-NP can enhance the catalytic activity of Au-NP for the 4-NP reduction due to the enrichment of reactant on Au-NP surface. On the other hand, the introduction of GNS further improves the catalytic activity of Au-NP due to the high conductivity of GNS and good dispersibility of Au-NP on the GNS surface. Due to the high catalytic activity of Au-NPs@NH₂/GNS-PO₃H₂ composites, we expect that the composites have wide applications in catalysis and environment fields.

Acknowledgements

This research was sponsored by National Natural Science Foundation of China (21301114), Natural Science Foundation of Shaanxi Province (2013JQ2009), and Fundamental Research Funds for the Central Universities (GK201503036).

Notes and references

- S. Dhar, W. L. Daniel, D. A. Giljohann, C. A. Mirkin and S. J. Lippard, *J. Am. Chem. Soc.*, 2009, **131**, 14652-14653.
- M. Zayats, E. Katz, R. Baron and I. Willner, *J. Am. Chem. Soc.*, 2005, **127**, 12400-12406.
- B. I. Ipe, K. Yoosaf and K. G. Thomas, *J. Am. Chem. Soc.*, 2006, **128**, 1907-1913.
- A. E. Prigodich, A. H. Alhasan and C. A. Mirkin, *J. Am. Chem. Soc.*, 2011, **133**, 2120-2123.
- A. Kumar, S. Huo, X. Zhang, J. Liu, A. Tan, S. Li, S. Jin, X. Xue, Y. Zhao, T. Ji, L. Han, H. Liu, X. Zhang, J. Zhang, G. Zou, T. Wang, S. Tang and X. J. Liang, *ACS Nano*, 2014, **8**, 4205-4220.
- M. Xiao, S. Li, X. Zhao, J. Zhu, M. Yin, C. Liu and W. Xing, *ChemCatChem*, 2014, **6**, 2825-2831.
- M. Wang, J. Ma, C. Chen, F. Lu, Z. Du, J. Cai and J. Xu, *Chem. Commun.*, 2012, **48**, 10404-10406.
- M. Wang, F. Wang, J. Ma, M. Li, Z. Zhang, Y. Wang, X. Zhang and J. Xu, *Chem. Commun.*, 2014, **50**, 292-294.
- S. Shi, C. Chen, M. Wang, J. Ma, H. Ma and J. Xu, *Chem. Commun.*, 2014, **50**, 9079-9082.
- B. Habibi and N. Delnavaz, *RSC Adv.*, 2015, **5**, 73639-73650.
- M. Veerapandian and S. Neethirajan, *RSC Adv.*, 2015, **5**, 75015-75024.
- Z. Ma, Y. Qiu, Y. Huang, F. Gao and P. Hu, *RSC Adv.*, 2015, **5**, 79456-79462.
- J. H. Min, S. Y. Jang, K. Y. Kim, S. B. Choi, W. S. Seong and D. S. Lee, *RSC Adv.*, 2015, **5**, 75325-75332.
- X. Chen, X. Tian, B. Su, Z. Huang, X. Chen and M. Oyama, *Dalton T.*, 2014, **43**, 7449-7454.
- Q. Wang, M. Song, C. Chen, W. Hu and X. Wang, *ChemPlusChem*, 2012, **77**, 432-436.
- G. R. Xu, J. J. Hui, T. Huang, Y. Chen and J.-M. Lee, *J. Power Sources*, 2015, **285**, 393-399.
- G. Fu, L. Tao, M. Zhang, Y. Chen, Y. Tang, J. Lin and T. Lu, *Nanoscale*, 2013, **5**, 8007-8014.
- J. Zhao, H. Li, Z. Liu, W. Hu, C. Zhao and D. Shi, *Carbon*, 2015, **87**, 116-127.
- K. Qu, L. Wu, J. Ren and X. Qu, *ACS Appl. Mater. Inter.*, 2012, **4**, 5001-5009.
- A. F. Zedan, S. Moussa, J. Ternner, G. Atkinson and M. S. F. Shall, *ACS Nano*, 2013, **7**, 627-636.
- G. R. S. Iyer, J. Wang, G. Wells, S. Gurusankar, S. Payne, I. Bradley and F. Borondics, *ACS Nano*, 2014, **8**, 6353-6362.
- H. Moon, D. Kumar, H. Kim, C. Sim, J. H. Chang, J. M. Kim, H. Kim and D. K. Lim, *ACS Nano*, 2015, **9**, 2711-2719.
- Z. Zhu, L. Ma, M. Su, D. Liu and Z. Wang, *J. Mater. Chem. B*, 2013, **1**, 1432-1438.
- Y. Qin, J. Li, Y. Kong, X. Li, Y. Tao, S. Li and Y. Wang, *Nanoscale*, 2014, **6**, 1281-1285.
- H. Yao, L. Jin, H. J. Sue, Y. Sumi and R. Nishimura, *J. Mater. Chem. A*, 2013, **1**, 10783-10789.
- Y. H. Lee, L. Polavarapu, N. Gao, P. Yuan and Q.-H. Xu, *Langmuir*, 2012, **28**, 321-326.
- J. Xiang and L. T. Drzal, *ACS Appl. Mater. Inter.*, 2011, **3**, 1325-1332.
- R. Lu, A. Konzelmann, F. Xu, Y. Gong, J. Liu, Q. Liu, M. Xin, R. Hui and J. Z. Wu, *Carbon*, 2015, **86**, 78-85.
- Y. Wang, L. Polavarapu and L. M. Liz-Marzán, *ACS Appl. Mater. Inter.*, 2014, **6**, 21798-21805.
- M. K. Chuang, S. W. Lin, F. C. Chen, C. W. Chu and C. S. Hsu, *Nanoscale*, 2014, **6**, 1573-1579.
- H. Yin, H. Tang, D. Wang, Y. Gao and Z. Tang, *ACS Nano*, 2012, **6**, 8288-8297.
- J. Zhou, M. Chen and G. Diao, *J. Mater. Chem. A*, 2013, **1**, 2278-2285.
- X. R. Li, X. L. Li, M. C. Xu, J. J. Xu and H. Y. Chen, *J. Mater. Chem. A*, 2014, **2**, 1697-1703.
- S. S. Li, A. J. Wang, Y. Y. Hu, K. M. Fang, J. R. Chen and J. J. Feng, *J. Mater. Chem. A*, 2014, **2**, 18177-18183.
- S. Xu, L. Yong and P. Wu, *ACS Appl. Mater. Inter.*, 2013, **5**, 654-662.
- Y. Ling, X. Li, S. Zhou, X. Wang and R. Sun, *J. Mater. Chem. A*, 2015, **3**, 7422-7428.
- K. Qu, L. Wu, J. Ren and X. Qu, *Nano Res.*, 2013, **6**, 693-702.
- Y. Zhang, G. M. Zeng, L. Tang, J. Chen, Y. Zhu, X. X. He and Y. He, *Anal. Chem.*, 2015, **87**, 989-996.
- J. Ju and W. Chen, *Anal. Chem.*, 2015, **87**, 1903-1910.
- P. Zhang, X. Zhang, S. Zhang, X. Lu, Q. Li, Z. Su and G. Wei, *J. Mater. Chem. B*, 2013, **1**, 6525-6531.
- Z. Juanjuan, L. Ruiyi, L. Zaijun, L. Junkang, G. Zhiguo and W. Guangli, *Nanoscale*, 2014, **6**, 5458-5466.
- G. Yang, L. Li, R. K. Rana and J. J. Zhu, *Carbon*, 2013, **61**, 357-366.
- J. Zhou, M. Chen, J. Xie and G. Diao, *ACS Appl. Mater. Inter.*, 2013, **5**, 11218-11224.
- D. Liu, L. Yang, J. S. Huang, Q. H. Guo and T. Y. You, *RSC Adv.*, 2014, **4**, 13733-13737.

45. X. Li, Y. Zhao, H. Wang, H. Tang, J. Tian and Y. Fan, *Mater. Chem. Phys.*, 2014, **144**, 107-113.
46. X. H. Zhou, X. R. Huang, L. H. Liu, X. Bai and H. C. Shi, *RSC Adv.*, 2013, **3**, 18036-18043.
47. Z. Jiang, Y. Shi, Z. J. Jiang, X. Tian, L. Luo and W. Chen, *J. Mater. Chem. A*, 2014, **2**, 6494-6503.
48. S. Zhou, D. Wei, H. Shi, X. Feng, K. Xue, F. Zhang and W. Song, *Talanta*, 2013, **107**, 349-355.
49. D. S. Yu, T. Kuila, N. H. Kim, P. Khanra and J. H. Lee, *Carbon*, 2013, **54**, 310-322.
50. J. S. Yeo, J. M. Yun, Y. S. Jung, D. Y. Kim, Y. J. Noh, S. S. Kim and S. I. Na, *J. Mater. Chem. A*, 2014, **2**, 292-298.
51. J. Li, G. Xiao, C. Chen, R. Li and D. Yan, *J. Mater. Chem. A*, 2013, **1**, 1481-1487.
52. Y. Kuang, J. Chen, X. Zheng, X. Zhang, Q. Zhou and C. Lu, *Nanotechnology*, 2013, **24**, 395604.
53. P. Li, H. Liu, Y. Ding, Y. Wang, Y. Chen, Y. Zhou, Y. Tang, H. Wei, C. Cai and T. Lu, *J. Mater. Chem.*, 2012, **22**, 15370-15378.
54. Y. Chen, X. J. Yang, B. Jin, L. R. Guo, L. M. Zheng and X. H. Xia, *J. Phys. Chem. C*, 2009, **113**, 4515-4521.
55. Y. Chen, B. Jin, L. R. Guo, X. J. Yang, W. Chen, G. Gu, L. M. Zheng and X. H. Xia, *Chem-Eur J.*, 2008, **14**, 10727-10734.
56. Y. Brahmī, N. Katir, J. A. M. Agullo, A. Primo, M. Bousmina, J. P. Majoral, H. Garcia and A. El Kadib, *Dalton T.*, 2015, **44**, 15544-15556.
57. P. S. da Silva, B. C. Gasparini, H. A. Magosso and A. Spinelli, *J. Hazard. Mater.*, 2014, **273**, 70-77.
58. V. Evangelista, B. Acosta, S. Miridonov, E. Smolentseva, S. Fuentes and A. Simakov, *Appl. Catal. B-Environ.*, 2015, **166-167**, 518-528.
59. Z. Dong, X. Le, C. Dong, W. Zhang, X. Li and J. Ma, *Appl. Catal. B-Environ.*, 2015, **162**, 372-380.
60. J. Zhang, G. Chen, M. Chaker, F. Rosei and D. Ma, *Appl. Catal. B-Environ.*, 2013, **132-133**, 107-115.
61. K. Dong, Z. Liu and J. Ren, *CrystEngComm*, 2013, **15**, 6329-6334.
62. S. Li, S. Guo, H. Yang, G. Gou, R. Ren, J. Li, Z. Dong, J. Jin and J. Ma, *J. Hazard. Mater.*, 2014, **270**, 11-17.
63. M. Liang, L. Wang, R. Su, W. Qi, M. Wang, Y. Yu and Z. He, *Catal. Sci. Technol.*, 2013, **3**, 1910-1914.
64. H. G. Lee, G. Sai Anand, S. Komathi, A. I. Gopalan, S. W. Kang and K. P. Lee, *J. Hazard. Mater.*, 2015, **283**, 400-409.
65. B. K. Barman and K. K. Nanda, *Dalton T.*, 2015, **44**, 4215-4222.
66. Y. Jia, Y. Yang, Y. Guo, W. Guo, Q. Qin, X. Yang and Y. Guo, *Dalton T.*, 2015, **44**, 9439-9449.
67. M. M. Nigra, J. M. Ha and A. Katz, *Catal. Sci. Technol.*, 2013, **3**, 2976-2983.
68. X. Yang, J. Wang, D. Su, Q. Xia, F. Chai, C. Wang and F. Qu, *Dalton T.*, 2014, **43**, 10057-10063.
69. P. CooperáStevenson, *Discuss. Faraday Soc.*, 1951, **11**, 55-75.
70. M. Yamamoto, Y. Kashiwagi, T. Sakata, H. Mori and M. Nakamoto, *Chem. Lett.*, 2007, **36**, 1348-1349.
71. L. Zhou, X. Lin, T. Huang and A. Yu, *J. Mater. Chem. A*, 2014, **2**, 5117-5123.
72. A. Ojida, M. Inoue, Y. Mito-oka, H. Tsutsumi, K. Sada and I. Hamachi, *J. Am. Chem. Soc.*, 2006, **128**, 2052-2058.
73. L. N. Johnson and R. J. Lewis, *Chem. Rev.*, 2001, **101**, 2209-2242.
74. S. Anderson, U. Neidlein, V. Gramlich and F. Diederich, *Angew. Chem. Int. Edit.*, 1995, **34**, 1596-1600.
75. R. Ren, S. Li, J. Li, J. Ma, H. Liu and J. Ma, *Catal. Sci. Technol.*, 2015, **5**, 2149-2156.
76. Y. Zhang, S. Liu, W. Lu, L. Wang, J. Tian and X. Sun, *Catal. Sci. Technol.*, 2011, **1**, 1142-1144.
77. J. Zhou and Q. Yang, *Chem. Asian J.*, 2012, **7**, 2045-2050.
78. F. Coccia, L. Tonucci, D. Bosco, M. Bressan and N. d'Alessandro, *Green Chem.*, 2012, **14**, 1073-1078.
79. J. Kou, C. Bennett-Stamper and R. S. Varma, *ACS Sustain. Chem. Eng.*, 2013, **1**, 810-816.
80. S. Sarkar, A. K. Sinha, M. Pradhan, M. Basu, Y. Negishi and T. Pal, *J. Phys. Chem. C*, 2010, **115**, 1659-1673.
81. G. Fu, L. Ding, Y. Chen, J. Lin, Y. Tang and T. Lu, *Crystengcomm*, 2014, **16**, 1606-1610.
82. M. Wang, F. Wang, J. Ma, C. Chen, S. Shi and J. Xu, *Chem. Commun.*, 2013, **49**, 6623-6625.